

See discussions, stats, and author profiles for this publication at: <https://www.researchgate.net/publication/23807854>

# Interactions between DMPC liposomes and the serum blood proteins HSA and IgG

ARTICLE in THE JOURNAL OF PHYSICAL CHEMISTRY B · FEBRUARY 2009

Impact Factor: 3.3 · DOI: 10.1021/jp804641e · Source: PubMed

CITATIONS

25

READS

132

## 8 AUTHORS, INCLUDING:



**Xerardo Prieto**

University of Santiago de Compostela

111 PUBLICATIONS 1,677 CITATIONS

SEE PROFILE



**Juan M. Ruso**

University of Santiago de Compostela

163 PUBLICATIONS 2,042 CITATIONS

SEE PROFILE



**Paula V Messina**

Universidad Nacional del Sur

75 PUBLICATIONS 634 CITATIONS

SEE PROFILE



**Miguel Costas**

Universidad Nacional Autónoma de México

105 PUBLICATIONS 2,066 CITATIONS

SEE PROFILE

## Interactions between DMPC Liposomes and the Serum Blood Proteins HSA and IgG

Juan Sabín,<sup>†</sup> Gerardo Prieto,<sup>†</sup> Juan M. Ruso,<sup>†</sup> Paula V. Messina,<sup>‡</sup> Francisco J. Salgado,<sup>§</sup> Montserrat Nogueira,<sup>§</sup> Miguel Costas,<sup>\*,||</sup> and Félix Sarmiento<sup>\*,†</sup>

*Grupo de Biofísica e Interfases, Departamento de Física Aplicada, Facultad de Física, Universidad de Santiago de Compostela, 15782-Santiago de Compostela, Spain; Departamento de Química, Universidad Nacional del Sur, 8000 Bahía Blanca, Argentina; Departamento de Bioquímica y Biología Molecular, Facultad de Biología, Universidad de Santiago de Compostela, 15782-Santiago de Compostela, Spain; and Laboratorio de Biofisicoquímica, Departamento de Fisicoquímica, Facultad de Química, Universidad Nacional Autónoma de México, Cd. Universitaria, México D.F. 04510, México*

Received: May 26, 2008; Revised Manuscript Received: December 10, 2008

The interaction between two serum blood proteins, namely human serum albumin (HSA) and human immunoglobulin G (IgG), with 1,2-dimyristoyl-*sn*-glycero-3-phosphatidylcholine (DMPC) liposomes has been studied in detail using dynamic light scattering, flow cytometry, enzyme-linked immunosorbent assay (ELISA), electrophoretic mobility, differential scanning calorimetry (DSC), and surface tension measurements. HSA and IgG interact with liposomes forming molecular aggregates that remain stable at protein concentrations beyond those of total liposome coverage. Both HSA and IgG penetrate into the liposome bilayer. An ELISA assay indicates that the Fc region of IgG is the one that is immersed in the DMPC membrane. The liposome–protein interaction is mainly of electrostatic nature, but an important hydrophobic contribution is also present.

## Introduction

Liposomes can be described as colloids of association, built up of double-chained lipids that self-assemble in aqueous media into spherical closed structures. Owing to their size, amphiphilic character, and biocompatibility, they are promising systems for drug delivery through the bloodstream.<sup>1</sup> To further advance this biomedical application,<sup>2,3</sup> it is important to characterize the interactions between liposomes and blood components, particularly with serum proteins that play an important role in the stability and properties of liposomes in blood e.g. in their circulation lifetimes.<sup>4,5</sup>

Liposome–protein interactions have been studied for several systems employing numerous techniques. The available data regarding the interaction between human serum albumin (HSA) and lipid membranes have been reviewed and discussed.<sup>6</sup> It has been found that proteins partially penetrate<sup>7–10</sup> and deform the lipid bilayer<sup>11,12</sup> when they are in contact with the membrane surface. This protein penetration into the liposomal membrane can change the properties of the bilayer with drastic consequences in their use as drug delivery systems. For example, leakage of the entrapped content is better prevented when egg yolk phosphatidylcholine (EYPC) liposomes are coated with bovine serum albumin (BSA),<sup>8,9</sup> a reduction of counterions mobility is produced by the interaction of BSA on EYPC liposomes,<sup>13</sup> and a thinning of the effective membrane thickness of protein-coated liposomes together with a reduction of the layer spacing in a stack of membranes in multilamellar liposomes have been theoretically predicted.<sup>14</sup>

It has been found that liposomes or liposome aggregates with diameters bigger than 0.1  $\mu\text{m}$  are removed from the bloodstream by cells of the mononuclear phagocytic system.<sup>15</sup> Therefore, small and stable liposome systems are suitable for drug delivery since they are cleared slowly from blood circulation and are less avidly sequestered by the liver.<sup>16</sup> On the other hand, liposomes larger than 0.1  $\mu\text{m}$  can also be used as drug delivery systems<sup>17</sup> by attaching polymers such as poly(ethylene glycol) or poloxamer to the membrane, reducing the affinity of particles for mononuclear phagocyte system (MPS) cells and hence prolonging the circulation time. Owing to these findings, the study of the stability of liposomes in the presence of proteins is also very important for their biomedical applications. Liposome flocculation has been examined as a function of liposome size,<sup>18</sup> temperature,<sup>19,20</sup> and ligand adsorption on liposome surface.<sup>21,22</sup> Regarding the mechanism involved in flocculation, EYPC liposomes partially covered by globular proteins aggregate by a bridging mechanism at protein concentrations around 1 mg mL<sup>-1</sup>.<sup>23</sup>

Many water-soluble proteins when interact with plasma or intracellular membranes undergo large structural changes. The nature of these conformational changes is a central issue to understand the problem of protein folding in membrane environments. For example, the association with negatively charged membranes induces a conformational change within  $\alpha$ -lactalbumin to a flexible, molten globule-like state.<sup>24</sup> Evidence that the structure of the membrane-bound protein can be altered by changes of the lipid bilayer offers a possible mechanism by which information about the physical properties of a lipid bilayer could be transmitted to the membrane-associated proteins and likely affect their biological activity.<sup>25</sup>

Using a variety of experimental techniques, in this work we studied the interaction of two serum blood proteins, namely human serum albumin (HSA) and human immunoglobulin G (IgG), with 1,2-dimyristoyl-*sn*-glycero-3-phosphatidylcholine

\* Corresponding authors. E-mail: costasmi@servidor.unam.mx (M.C.); felix.sarmiento@usc.es (F.S.).

<sup>†</sup> Universidad de Santiago de Compostela.

<sup>‡</sup> Universidad Nacional del Sur.

<sup>§</sup> Universidad de Santiago de Compostela.

<sup>||</sup> Universidad Nacional Autónoma de México.

(DMPC) liposomes and monolayers, providing new evidence of the penetration of these proteins into the lipid structures. The stability of the liposome–protein systems has also been experimentally characterized and discussed in terms of the forces involved.

## Experimental Methods

**Liposomes Preparation.** 1,2-Dimyristoyl-*sn*-glycero-3-phosphatidylcholine (DMPC) with purity >99% was from Sigma and used without further purification. Organic solvents methanol and chloroform were from Aldrich and Merck, respectively. LUVs (large unilamellar vesicles) were prepared by the thin-film hydration method.<sup>25</sup> A solution of lipids (DMPC) in 1:4 (v/v) chloroform:methanol mixtures was evaporated to dryness under nitrogen flux, and the resulting lipid film was hydrated with double distilled water. This mixture was extruded (five times through each filter) using polycarbonate filters (Millipore) of 800, 400, and 200 nm pore size to form the LUVs. A homogeneous liposomal suspension of unilamellar liposomes was obtained. Lipids were usually dried under vacuum overnight. Extrusion was carried out above 23.5 °C, which is the phase transition temperature of DMPC.<sup>26</sup>

**IgG Purification.** Human serum was collected from healthy donors and stored at −20 °C until used. Samples of 1 mL were defrosted and centrifuged at 4 °C for 15 min at 13000g, and supernatant was gently mixed with 37 mg of potassium sulfate using soft shaking. After centrifugation at 13000g for 15 min, supernatant was carefully collected and filtered by using a 0.22  $\mu$ m filter (Amicon). To select the IgG, a T-Gell adsorbent column (Pierce) was used according to the manufacturer's instructions with modifications in order to optimize the quantitative and qualitative yield. The sample, 1 mL of serum 0.5 M potassium sulfate, was loaded in a T-Gell column previously equilibrated with binding buffer (Pierce) at room temperature. After washing with 15 mL of binding buffer, immunoglobulins were eluted with 10 mL of elution buffer and fractions of 3 mL were collected. The elution of IgG was followed at 280 nm corresponding the maxima absorbance to the fraction 2. 1 mL of this fraction 2 was rechromatographed at the same conditions, and again fraction 2 showed the maxima absorbance. The amount of protein bound to the matrix was determined by a BCA test according the manufacturer's instructions. Routinely, 12% of total protein from serum sample was bound to the matrix. This represents the 90% of the standardized amount of immunoglobulins present in healthy human blood. To set the qualitative and quantitative IgG yield, rechromatographed fraction 2 was analyzed by dimensional electrophoresis and staining. Purified IgG was dialyzed against Milli-Q water and aliquots of 1 mg/mL stored at −20 °C. IgG stock solution (1 mg mL<sup>−1</sup>) was obtained from the previous described method. Solutions were kept in refrigerator before use (−20 °C) and diluted as required. IgG solutions were prepared without buffer addition since its presence could affect surface tension measurements.

**Sample Preparation.** All experiments were performed using solutions that were prepared mixing aqueous solutions of stable LUVs and protein (HSA or IgG) at different concentrations. Human serum albumin, HSA (albumin  $\geq$ 96%, essentially fatty acid free), was from Sigma Chemical Co. For most experiments, the DMPC concentration was 0.5 mM and the protein concentration 0.125 mg mL<sup>−1</sup>. To obtain accurate data, some experiments required higher or lower concentrations. However, in all cases the lipid/protein concentration ratio was kept constant,

265 for DMPC/HSA and 602 for DMPC/IgG. Except for ELISA and flow cytometry assays, the use of buffers was avoided.

**Dynamic Light Scattering.** Measurements of the size and polydispersities of the liposomes systems were made by dynamic light scattering (DLS) at 25 °C using a spectrometer (Autosizer 4800, Malvern Instruments) whose detection range is 1–5000 nm. This instrument is equipped with a Uniphase 75 mW Ar laser operating at 488 nm with vertically polarized light at a scattering angle of 90°. Time correlation was analyzed by a digital autocorrelator PCS7132 from Malvern Instruments and using the CONTIN algorithm. A Malvern Nano S apparatus with a noninvasive backscattering (NIBS) laser technology was used to determine the size distribution of protein, liposomes, and protein–liposome systems. A 50 mW laser operating at 532 nm was employed with a Peltier controller to keep temperature constant.

**Electrophoretic Mobility.** Zeta potentials ( $\zeta$ -potentials) of the liposome systems were measured using a Malvern Instruments Zetamaster 5002. For all samples, an average of five measurements at stationary level was taken. The cell used was a 5  $\times$  2 mm rectangular quartz capillary. The temperature was kept constant by a Haake temperature controller. The zeta potential was calculated from the electrophoretic mobility,  $\mu_E$ , using the Henry correction to Smoluchowski's equation.

**Differential Scanning Calorimetry (DSC).** DSC measurements were performed using a MicroCal VP-DSC differential scanning calorimeter (MicroCal, Inc.) with a cell volume of 0.514 mL. Prior to each scan, samples were equilibrated at 5 °C for 1 h. The heating rate was 1 °C min<sup>−1</sup>. Scans were performed for DMPC liposomes in the absence and presence of HSA and IgG at 0.125 and 0.25 mg mL<sup>−1</sup>. At least three calorimetric scans were performed for each sample (same liposome preparation, different calorimeter fillings). Very good reproducibility was observed, namely the temperatures where the maxima in the calorimetric traces occur (pre- and main transitions), and the area under the peaks varied within 0.05 °C and 0.1 kcal mol<sup>−1</sup>, respectively. Data evaluation was performed using the Origin 5.0 software package.

**Enzyme-Linked Immunosorbent Assay (ELISA).** ELISA wells were coated or not with liposomes or IgG–liposome molecular aggregates (obtained as indicated above) according to Aguilar et al.<sup>27</sup> Some modifications were employed. Both liposomes and IgG–liposome systems were resuspended (1 mM) in a buffer solution at pH 7 (TBS), and after 2 h incubation at 25 °C the blocking solution [gelatin in TBS (0.4% w:v)] was added to each well of the microtiter plate. After washing, blocked wells were incubated with antihuman IgG (Fc specific)–peroxidase or antihuman IgG (Fab specific)–peroxidase diluted in TBS buffer (from 1:2000 to 1:100). Bound antibodies were detected by reaction with *o*-phenylenediamine dihydrochloride, and the absorbance was measured at 450 nm using a Labsystem Multiskan MS.

**Flow Cytometry.** As with cells,<sup>28,29</sup> the diffraction of the laser beam (forward scatter, FSC) is proportional to the liposome size while refraction plus reflection of the beam (side scatter, SSC) is proportional to the complexity of the liposome. The quantification of both FSC and SSC was performed using a FACScalibur flow cytometer (Becton Dickinson, San Jose, CA), equipped with a 15 mW 488 nm air-cooled argon ion laser. Prior to the flow cytometry analysis, liposomes with and without IgG were washed twice in TBS pH 7.0 and finally resuspended in the same buffer at a concentration of 0.5 mM. To accommodate the entire liposome size range, both forward and side scatter were set to a logarithmic amplification mode. A constant

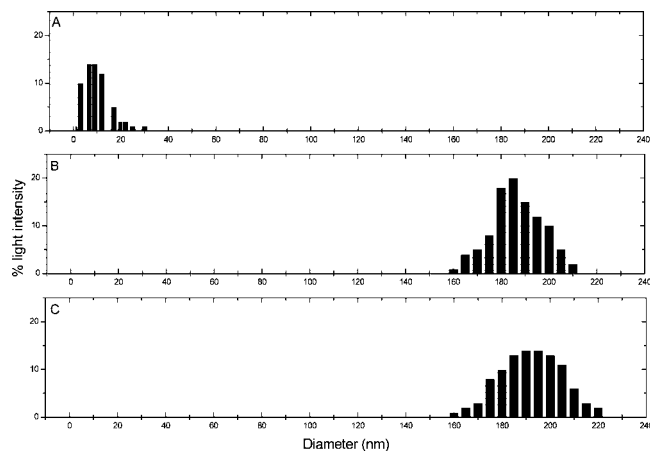


**Figure 1.** Diameter distribution in a pure HSA ( $0.125 \text{ mg mL}^{-1}$ ) solution (A), a DMPC liposomes ( $0.5 \text{ mM}$ ) solution (B), and a mixture of both (C). At the HSA concentration used in (A), there is no protein aggregation.

SSC detector voltage of 650 V was used, while the FSC detector was set to either E01 or E02. During these experiments, 20000 events were collected at three different rates. The data were analyzed using the WinMDI software.

**Surface Tension Measurements.** The experiments were performed with a constant pressure penetration Langmuir balance based on axisymmetric drop shape analysis (ADSA). Details of this instrument can be found in ref 30. The whole setup, including the image capturing device, the microinjector, the ADSA algorithm, and the fuzzy pressure control, is controlled by a Windows integrated program (DINATEM). A solution droplet is formed at the tip of the coaxial double capillary, connected to a double microinjector. During the experiment, the sample solution forms a pendant drop at the tip of a capillary, enclosed in a quartz cuvette which is mounted in an environmental chamber. DMPC was dissolved in a 1:4 (v/v) methanol:chloroform mixture to obtain  $1 \times 10^{-5} \text{ M}$  final lipid concentration solutions. An aliquot of  $4.0 \mu\text{L}$  was spread on the subphase using a microsyringe. The DMPC solutions were spread onto a cleaned surface of a water drop where a monolayer is formed. Subsequently, the water subphase was exchanged by a protein solution. 4 min was allowed for solvent evaporation. The experimental drop profiles, extracted from digital drops micrographs, were fitted to the Young–Laplace equation for capillarity using ADSA which provides as outputs the drop volume  $V$ , the interfacial tension  $\gamma$ , and the surface area  $A$ . Pressure and area, which can be modified changing the drop volume, are controlled using a modulated fuzzy logic PID algorithm (proportional, integral, and derivative control).

## Results and Discussion

### Formation and Stability of Liposome–Protein Systems.

The particle size distribution in a HSA + water solution, a DMPC liposomes solution, and a mixture of both were determined employing light scattering, the results being displayed in Figure 1. The mean diameter of HSA is 6.5 nm, in agreement with the reported hydrodynamic diameter.<sup>31,32</sup> The highest value for 20% light intensity for DMPC liposomes was 185 nm, as expected from the pore size of the filters (200 nm) employed in their preparation.<sup>33,34</sup> When the HSA and DMPC liposome solutions are mixed, only one population centered at 195 nm is detected. This suggests that liposome–HSA molecular aggregates are formed in the bilayer surface and that all the HSA present is involved in that event.

To analyze DMPC–liposome–IgG systems, flow cytometry was employed (Figure 2). This technique allows us to count, examine, and sort microscopic particles suspended in a stream of fluid, performing a simultaneous multiparametric analysis of physical characteristics of single cells (liposomes) flowing through an optical and/or electronic detection apparatus. As can be seen in Figure 2A, the analysis of DMPC liposomes shows a population with a well-defined ratio forward/side scatters (equivalent to a size/complexity scatter ratio). When IgG is added to the liposomes (Figure 2B), a significant change in relation with diffraction (forward scatter) and refraction plus reflection of the laser beam (side scatter) is observed. This change makes evident the existence of a more heterogeneous population, indicating the presence of liposome–IgG systems.

The forces that are involved in the interaction between the liposomes and the proteins are of electrostatic and hydrophobic nature. Since the zeta potential ( $\zeta$ ) is proportional to the surface charge density, it can be used to monitor the attractive electrostatic contribution to the binding of the negatively charged proteins (at the employed pH = 7) to the positively charged liposome surface. Figure 3 displays the liposome zeta potentials as a function of HSA and IgG concentration. For other liposome–protein systems, a decrease of  $\zeta$  with protein concentration have also been found and attributed to protein adsorption.<sup>13</sup> The  $\zeta$  values in Figure 3 decrease exponentially with protein concentration, reaching zero at  $\sim 0.15 \text{ mg mL}^{-1}$  for HSA and  $0.125 \text{ mg mL}^{-1}$  for IgG. The strong dependence of  $\zeta$  with protein concentration is patent evidence that the attractive electrostatic contribution to the formation of the DMPC liposomes–(HSA or IgG) systems is of major importance. At the protein concentrations where the zeta potential is zero, the total liposome surface area is covered. Assuming monodisperse DMPC liposomes with 170 nm of diameter and 4 nm of bilayer width, for a DMPC concentration of 0.5 mM in a 1 mL sample the total external area is  $\sim 0.107 \text{ m}^2$ . The hydrodynamic radius necessary to cover this liposome area at the concentrations where  $\zeta = 0$  are 2.5 nm for HSA and 4.2 nm for IgG. These diameters are close to the reported hydrodynamic radius of 3.3 nm for HSA<sup>31,32</sup> and 5.3 nm for IgG.<sup>36,37</sup> The fact that the calculated protein diameters are smaller than the hydrodynamic ones might be an indication that both HSA and IgG penetrate to some extent into the DMPC bilayer. They could also be interpreted as a signal for protein adsorption. However, the DSC and surface tension data discussed in the next section clearly support the protein penetration possibility.

The stability of the liposome–protein systems was evaluated measuring the polydispersity and diameter by dynamic light scattering. Following the classical DLVO theory,<sup>38,39</sup> the stability of colloid is governed by a repulsive electrostatic potential and an attractive van der Waals potential. When the surface charge of the liposome is screened, they undergo aggregation processes.<sup>40,41</sup> Figure 4 shows that the liposome–protein systems remain stable in a wide range of HSA and IgG concentrations. This suggests the existence of additional repulsive forces that avoid the aggregation of the liposomes covered by HSA and IgG. Steric forces can be the responsible of keeping the systems far enough to avoid the attraction caused by the van der Waals potential.<sup>42</sup>

**Protein Penetration into the Liposome Structure.** In order to test whether HSA and IgG penetrate into the DMPC membrane, lipid packing at the liposome bilayer was sensed using DSC. Representative calorimetric traces for DMPC liposomes in the absence and presence of the proteins are shown in Figure 5. In good agreement with literature, the temperature



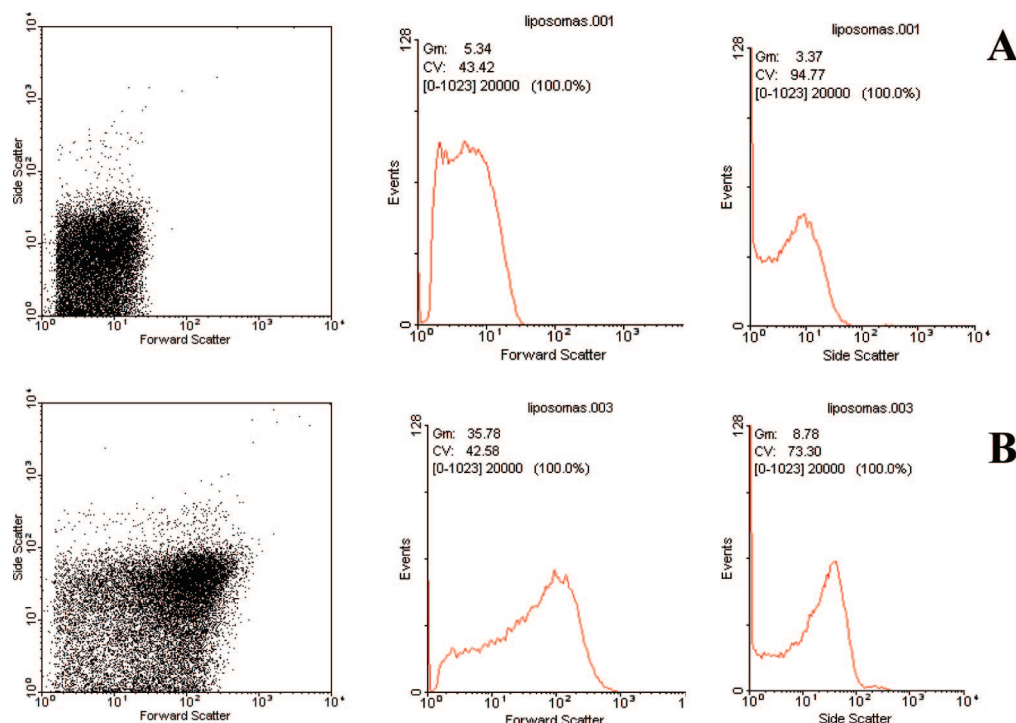


**Figure 2.** Flow cytometry results for DMPC liposomes (A) and liposomes in the presence of IgG (B). Data shown are representative of five independent experiments.

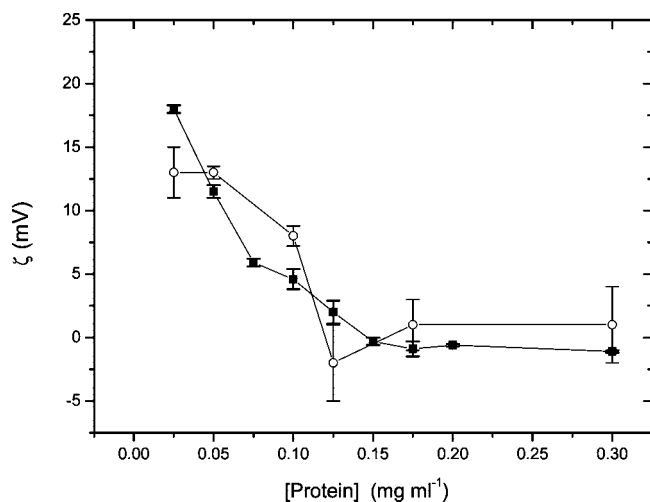


**Figure 3.** Zeta potential at 25 °C of a 0.5 mM DMPC liposomes solution as a function of (■) HSA and (○) IgG concentration.

and enthalpy of the main gel–liquid transition for DMPC liposomes were found to be 24.7 °C and 5.5 kcal mol<sup>-1</sup>, respectively. The so-called weak pretransition, concerning the mobility of the headgroup of the lipids, was also detected at 13.4 °C.<sup>26,43</sup> Inspection of Figure 5 inset suggests that the effect of both proteins on the pretransition temperature is similar, independently of the protein conformation (globular and non-globular). However, the observed effect is very small, affecting only the conformational flexibility of the external part of the liposome bilayer, i.e., the region where the phospholipids head groups are located. To conclude that such small effect will occur with other the proteins would require a larger study, covering many more proteins and complementary experimental techniques.

DSC scans were performed at two different concentrations (0.125 and 0.25 mg mL<sup>-1</sup>) of HSA and IgG, with similar results. Although the presence of the proteins produce changes in the transition temperatures and enthalpies that are small, these

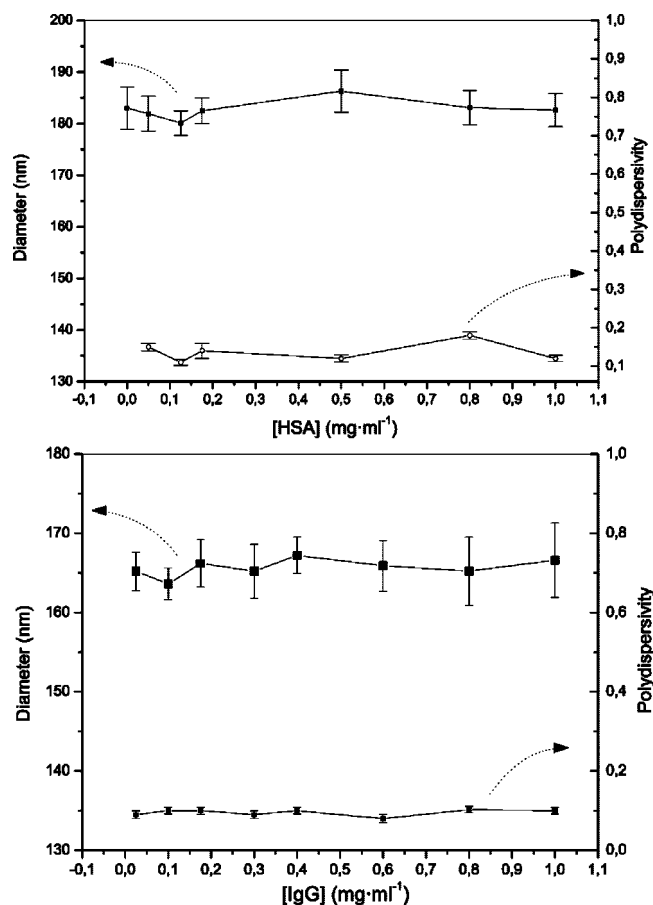


**Figure 4.** Mean diameter and polydispersity of DMPC liposomes in a wide range of HSA and IgG concentrations.

changes are much bigger than the reproducibility observed performing multiple scans (see Differential Scanning Calorimetry (DSC) section). Hence, it is possible to draw the following

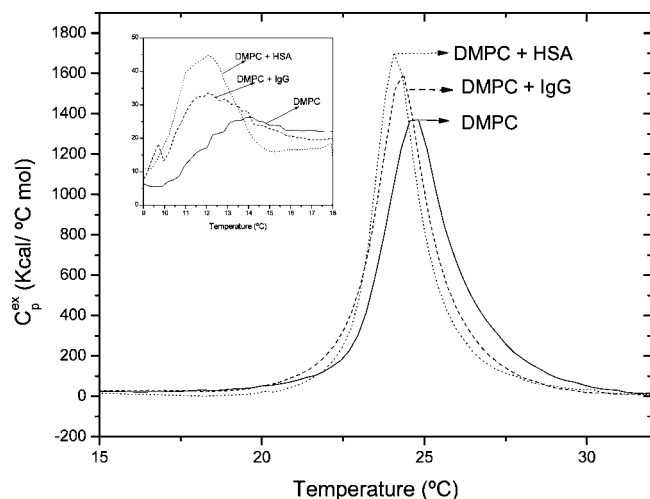


**Figure 5.** Representative DSC profiles for DMPC liposomes in the absence and presence of HSA and IgG (at 0.125 mg mL<sup>-1</sup>). Similar results were found at protein concentrations of 0.25 mg mL<sup>-1</sup> (data not shown). The inset shows the pretransitions in detail.

**TABLE 1: Transition Temperatures (in °C) and Enthalpies (in kcal mol<sup>-1</sup>) for DMPC in the Absence and in the Presence of HSA and IgG<sup>a</sup>**

	pretransition		main transition		
	<i>T<sub>m</sub></i>	$\Delta H$	<i>T<sub>m</sub></i>	$\Delta H$	$\Delta T_{1/2}^b$
DMPC	13.4	<0.1	24.7	5.5	2.3
DMPC + 0.125 mg mL <sup>-1</sup> HSA	12.1	0.35	24.1	5.4	1.6
DMPC + 0.25 mg mL <sup>-1</sup> HSA	12.0	0.26	24.0	5.2	1.6
DMPC + 0.125 mg mL <sup>-1</sup> IgG	12.1	0.30	24.3	5.6	1.9
DMPC + 0.25 mg mL <sup>-1</sup> IgG	12.2	0.28	24.2	5.7	1.8

<sup>a</sup> Average values obtained from at least three scans. <sup>b</sup> Peak width at half-peak area.

conclusion. The formation of liposome–protein systems decreases the pretransition temperature by more than one degree and increases its  $\Delta H$  (see Table 1), indicating that both proteins exert a considerable effect on the mobility of the charged head group of DMPC molecules. Figure 5 also shows that the main transition, due to a change from a gel-like to a liquid-like packing of the hydrophobic tails of the lipids, is also affected by the presence of HSA or IgG. Table 1 shows that enthalpy remains practically unchanged, while  $\Delta T_{1/2}$  values are lower for the liposome–protein system. Then, the entropy change ( $\Delta H/\Delta T_{1/2}$ ) increases. This means that the packing of the lipids is disturbed within the bilayer, i.e., their order is reduced. We suggest that these changes are consistent with the proteins penetrating the phospholipid bilayers. Qualitatively similar results for the pretransition and main transition of a mixture of large and small unilamellar 1,2-dipalmitoyl-*sn*-glycero-3-phosphatidylcholine (DPPC) liposomes in the presence of HSA have been reported.<sup>6</sup> The effect of HSA and IgG over the main DMPC transition implies that these proteins penetrate into the hydrophobic bilayer affecting the packing of the hydrocarbon tails of the lipids. Hence, there is also an important hydrophobic contribution to the formation of the DMPC liposomes–(HSA or IgG) systems. This contribution is given by the interaction between the DMPC tails and those parts of HSA and IgG that penetrate into the liposome bilayer.

To confirm the penetration of the HSA and IgG into the hydrophobic region of the liposomes, the dynamic adsorption of the two proteins to DMPC monolayers at the air/water interface was determined by interfacial tension ( $\gamma$ ) as a function of time.

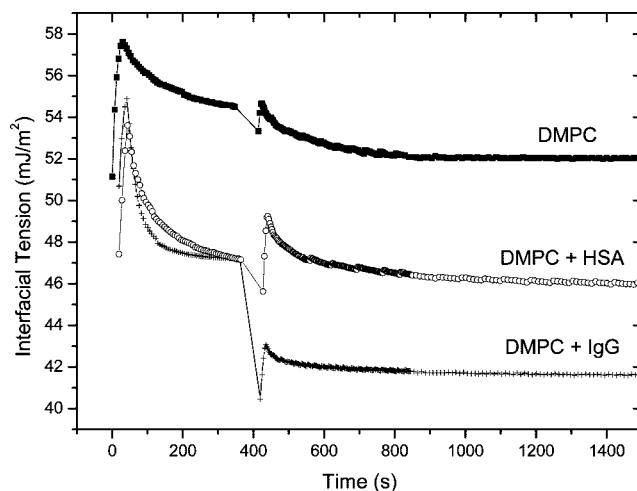


**Figure 6.** Dynamical interfacial tension ( $\gamma$ ) of DMPC spread monolayer with (■) water subphase, (+) 0.024 mg mL<sup>-1</sup> of IgG subphase, and (○) 0.024 mg mL<sup>-1</sup> of HSA subphase.

Figure 6 shows  $\gamma(t)$  of the monolayer with a subphase of 0.024 mg mL<sup>-1</sup> of HSA and IgG. The decrease of the interfacial tension when protein solution is injected on the subphase indicates that the protein molecules intercalate between the hydrophobic tails of the DMPC lipids. The hydrophobic regions of the proteins reduce the free energy by entering in the hydrocarbon region of the monolayer. Note that the  $\gamma$  decrease is more pronounced for IgG than for HSA. This is probably due to the structure of IgG (a Y shape) that facilitates its penetration into the monolayer while HSA, being essentially spherical, is somewhat hindered to access the lipid region of the monolayer. Taken together, the results in Figures 5 and 6 indicate that there is also an important hydrophobic contribution to the formation of the DMPC liposomes–(HSA or IgG) systems. This contribution is given by the interaction between the DMPC tails and those parts of HSA and IgG that penetrate into the liposome bilayer.

**HSA Conformational Changes upon Inclusion into the Liposomes.** The conformation of the proteins inserted in the membrane should be different from that in the solvent water. For HSA, this was examined by DSC. Figure 7 shows the DSC profile of HSA in the absence and in the presence of DMPC unilamellar liposomes. In these experiments, the HSA concentration was increased 10 times with respect to that used in all the other measurements, but the protein/lipid ratio was kept constant. Figure 7 indicates that the denaturation temperature for HSA in water (as measured by the temperature where the maximum of the calorimetric trace occurs) is 68.1 °C, in agreement with previous reports.<sup>44</sup> In the presence of DMPC liposomes, the HSA denaturation temperature decreases to 64.6 °C. This destabilization of the protein is similar to that seen when a protein is placed in the presence of small amounts of chemical denaturing agents such as urea. Hence, it can be concluded that HSA changes its conformation, albeit slightly, when interacting with the DMPC liposome. It would be interesting to find out whether this conformational change occurs at the secondary level structure of HSA. According to several studies in the literature,<sup>45–48</sup> this can be probably explored using circular dichroism. Work in this direction will be the subject of our near future research.

**IgG Orientation in the Liposomes.** IgG has a Y-shape form, the “upper branches” being termed Fab and the “vertical branch” Fc. To study the orientation of IgG in the DMPC liposome, the ELISA assay technique was used. Results from ELISA assays

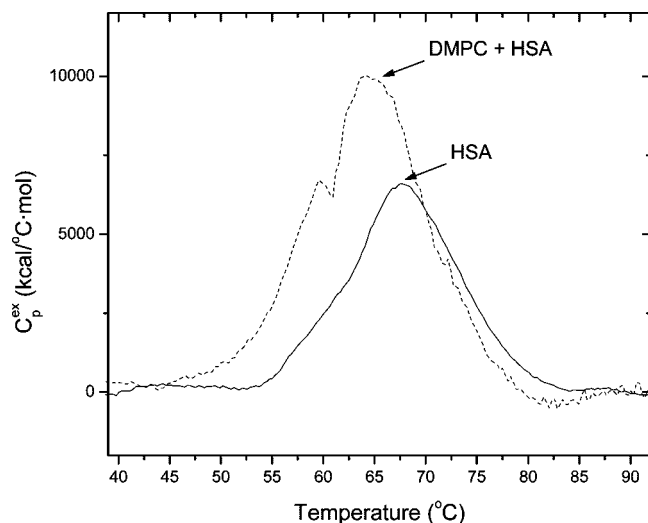


**Figure 7.** DSC profiles for HSA denaturation in the absence and presence of the DMPC liposomes. The HSA concentration was 1.25 mg mL<sup>-1</sup>, and the DMPC concentration was 5 mM.

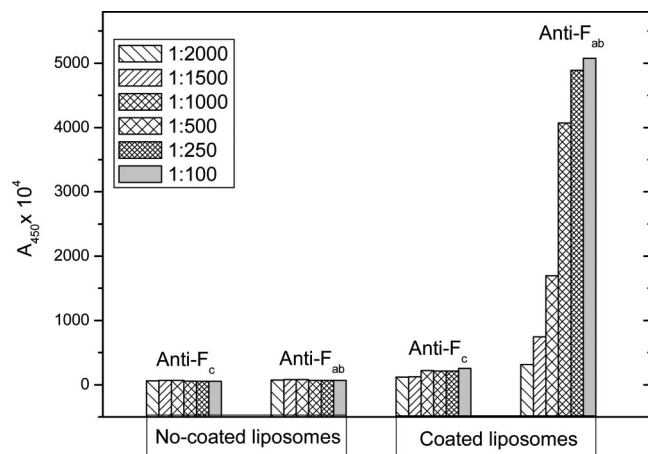


**Figure 8.** ELISA assay results. Absorbance values at 450 nm of noncoated and coated DMPC liposomes with anti-IgG (F<sub>c</sub> specific)–peroxidase or anti-IgG (F<sub>ab</sub> specific)–peroxidase. Absorbance values are shown at several dilutions in TBS.

using specific anti-Fab and anti-Fc antibodies are shown in Figure 8. When coated liposomes were incubated with anti-Fab, the absorbance values are bigger (a factor of 25 at the lowest anti-Fab dilution) than those observed when incubating with anti-Fc. Therefore, it is the Fc region of IgG the one that penetrates into the DMPC membrane. This conclusion receives support from examination of the hydrophobicity of Fab and Fc. Using UnitProtKB, Pfam, and TMpred software (Expasy.org), the Fab and Fc IgGs hydrophobicity were estimated. Taking into account the IgGs variability (subclasses 1–4) but also its amino acid sequence homology (more than 95%), one Fab and Fc protein of each type was selected employing the Swissport database. In all cases, the Fc region turned out to be more hydrophobic than Fab.

### Concluding Remarks

The interaction between DMPC liposomes and two serum proteins, HSA and IgG, has been studied in detail with a variety of experimental techniques. The strong absorption of the proteins to the liposome surface observed by zeta-potential measurements indicates that the electrostatic forces govern the formation of liposome–protein systems. However, the dynamic surface ten-

sion results for the adsorption of HSA and IgG to DMPC monolayers indicates that hydrophobic interactions also play an important role. DSCs measurements allowed us to characterize the changes in (i) the phase transitions of the lipid bilayer and (ii) the denaturation of the HSA, when the liposome–protein systems are formed. These changes are caused by HSA and IgG penetration into the hydrophobic tails region of the lipid bilayer. For the Y-shaped IgG, the ELISA assay showed that it is “vertical branch” (Fc) of the protein, the one which penetrates into the lipid bilayer. The stability of the liposomes–protein systems was also studied, finding that they remain stable even when liposomes are completely covered by protein and the electrostatic repulsion is null. This suggests that steric forces keep the systems far enough to avoid the attraction caused by the van der Waals potential.

**Acknowledgment.** We thank Asunción Delgado for her comments on the manuscript. This work was supported by grants from the Spanish “Ministerio de Educación y Ciencia” (Projects MAT2005-02421 and BFU2006-09717), the “European Regional Development Fund (ERDF)”, the “Xunta de Galicia” (Project PGIDIT05PXIB20001PR), the “Consejo Nacional de Ciencia y Tecnología de México (CONACYT)” (Grant 49811-Q), and PAPIIT-UNAM (Grant IN105107). F.S. thanks the “Consellería de Educación e Ordenación Universitaria da Xunta de Galicia”, and J.M.R. thanks the “Dirección Xeral de Promoción Científica e Tecnolóxica do Sistema Universitario de Galicia” for financial support. P.V.M. (assistant researcher of CONICET) thanks the “Agencia Nacional de Promoción Científica y Tecnológica (ANPCyT) de la República Argentina” and the “Consejo Nacional de Investigaciones Científicas y Técnicas de la República Argentina (CONICET)” for financial support.

### References and Notes

- (1) Sahoo, S. K.; Labhasetwar, V. *Drug Discovery Today* **2003**, *8*, 1112–1120.
- (2) Shek, P. N. *Liposomes in Biomedical Applications*; Drug Targeting and Delivery Series; Harwood Academic Publishers: Singapore, 1995.
- (3) Zonneveld, G. M.; Crommelin, D. J. A. In *Liposomes as Drug Carriers: Recent Trends and Progress*; Gregoriadis, G., Ed.; John Wiley: Chichester, 1998; pp 795–817.
- (4) Panagi, Z.; Avgoustakis, K.; Evangelatos, G.; Ithakissios, D. S. *Int. J. Pharm.* **1999**, *176*, 203–207.
- (5) Chonn, A.; Semple, S. C.; Cullis, P. R. *J. Biol. Chem.* **1992**, *267*, 18759–18765.
- (6) Galantai, R.; Bárdos-Nagy, I. *Int. J. Pharm.* **2000**, *195*, 207–218.
- (7) Sweet, C.; Zull, J. E. *Biochim. Biophys. Acta* **1969**, *173*, 94–103.
- (8) Law, S. L.; Lo, W. Y.; Pai, S. H.; Tech, G. W.; Kou, F. Y. *Int. J. Pharm.* **1986**, *32*, 237–241.
- (9) Law, S. L.; Lo, W. Y.; Pai, S. H.; Tech, G. W. *Int. J. Pharm.* **1988**, *43*, 257–260.
- (10) Juliano, R. L.; Kimelberg, H. K.; Papahadjopoulos, D. *Biochim. Biophys. Acta* **1971**, *241*, 894–905.
- (11) Lis, L. J.; Kauffman, J. W.; Shriver, D. F. *Biochim. Biophys. Acta* **1976**, *436*, 513–522.
- (12) Hoekstra, D.; Scherphoft, G. *Biochim. Biophys. Acta* **1979**, *551*, 109–121.
- (13) Matsumura, H.; Svetlana, V. V.; Dimitrova, M. N. *Colloids Surf., A* **2001**, *192*, 331–336.
- (14) Chen, C. M. *Physica A* **2000**, *281*, 41–50.
- (15) Szoka, F. C. *Biotech. Appl. Biochem.* **1990**, *12*, 496–500.
- (16) Armengol, X.; Estelrich, J. *J. Microencapsulation* **1995**, *12*, 525–535.
- (17) Kibanov, A. L.; Huang, L. *J. Lipid Res.* **1992**, *2*:3, 321–334.
- (18) Dimitrova, M. N.; Tsekov, R.; Matsumura, H.; Furusawa, K. *J. Colloid Interface Sci.* **2000**, *226*, 44–50.
- (19) Dimitrova, M. N.; Matsumura, H.; Neitchev, V. Z.; Furusawa, K. *Langmuir* **1998**, *14*, 5438–5445.
- (20) Schenkman, S.; Araujo, P.; Dukman, R.; Quina, F. H.; Chaimovich, H. *Biochim. Biophys. Acta* **1981**, *649*, 633–641.
- (21) Lynch, N.; Kilpatrick, P.; Carbonell, R. G. *Biotechnol. Bioeng.* **1996**, *50*, 151–168.

- (22) Lynch, N.; Kilpatrick, P.; Carbonell, R. G. *Biotechnol. Bioeng.* **1996**, *50*, 169–183.
- (23) Dimitrova, M. N.; Matsumura, H.; Neitchev, V. Z. *Langmuir* **1997**, *13*, 6516–6523.
- (24) Bañuelos, S.; Muga, A. *J. Biol. Chem.* **1995**, *270*, 29910–29915.
- (25) Bañuelos, S.; Muga, A. *FEBS Lett.* **1996**, *386*, 21–25.
- (26) Lasic, D. D. *Liposomes: from Physics to Applications*; Elsevier: Amsterdam, 1993.
- (27) Aguilar, L.; Ortega-Pierres, G.; Campos, B.; Fonseca, R.; Ibañez, M.; Wong, C.; Farfan, N.; Naciff, J. M.; Kaetzel, M. A.; Dedman, J. R.; Baeza, I. *J. Mol. Biol.* **1999**, *274*, 25193–25196.
- (28) Salgado, F. J.; Lojo, J.; Alonso-Lebrero, J. L.; Lluís, C.; Franco, R.; Cordero, O. J.; Nogueira, M. *J. Biol. Chem.* **2003**, *278*, 24849–24857.
- (29) Salgado, F. J.; Piñeiro, A.; Canda-Sánchez, A.; Lojo, J.; Nogueira, M. *Mol. Membr. Biol.* **2005**, *22*, 163–76.
- (30) Maldonado-Valderrama, J.; Wege, H. A.; Rodríguez-Valverde, M. A.; Galvez-Ruiz, M. J.; Cabrerizo-Vilchez, M. A. *Langmuir* **2003**, *19*, 8436–8442.
- (31) Cannistraro, S.; Sacchetti, F. *Phys. Rev. A* **1986**, *33*, 745–746.
- (32) Peters, T. J. *All about Albumin: Biochemistry, Genetics and Medical Applications*; Academic Press: San Diego, 1996.
- (33) Hunter, D. G.; Frisken, B. J. *Biophys. J.* **1998**, *74*, 2996–3002.
- (34) Mayer, L. D.; Hope, M. J.; Cullis, P. R. *Biochim. Biophys. Acta* **1986**, *858*, 161–168.
- (35) Casals, E.; Galán, A. M.; Escolar, G.; Gallardo, M.; Estelrich, J. *Chem. Phys. Lipids* **2003**, *125*, 139–146.
- (36) Feder, J.; Jøssang, T.; Rosenqvist, E. *Phys. Rev. Lett.* **1984**, *53*, 1403–1406.
- (37) Armstrong, J. K.; Wenby, R. B.; Meiselman, H. J.; Fisher, T. C. *Biophys. J.* **2004**, *87*, 4259–4270.
- (38) Derjaguin, B. V.; Landau, L. D. *Acta Physicochim. URSS* **1941**, *14*, 633–662.
- (39) Verwey, E. J. W.; Overbeek, J. Th. G. *Theory of the Stability of Lyophobic Colloids. The Interaction of Particles Having an Electric Double Layer*; Elsevier: Amsterdam, 1948.
- (40) Behrens, S. H.; Christl, D. I.; Emmerzael, R.; Schurtenberger, P.; Borkovec, M. *Langmuir* **2000**, *16*, 2566–2575.
- (41) Sabin, J.; Prieto, G.; Sennato, S.; Ruso, J. M.; Angelini, R.; Bordini, F.; Sarmiento, F. *Phys. Rev. E* **2006**, *74*, 031913-1–031913-7.
- (42) Elimelech, M.; Gregory, J.; Jia, X.; Williams, R. A. *Particle Deposition and Aggregation: Measurement, Modelling and Simulation*; Butterworth-Heinemann: Oxford, 1998.
- (43) Heerklotz, H.; Seelig, J. *Biophys. J.* **2002**, *82*, 445–452.
- (44) Gorinstein, S.; Weisz, M.; Caspi, A.; Libman, I.; Lerner, H. T.; Trakhtenberg, S.; Rosen, A.; Goshev, I.; Zemser, M.; Añón, M. C. *J. Pept. Res.* **2002**, *59*, 71–78.
- (45) Qi, X.; Grabowski, A. *Biochemistry* **1998**, *37*, 11544–11554.
- (46) Rueping, M.; Dietrich, A.; Buschmann, V.; Fritz, M. G.; Sauer, M.; Seebach, D. *Macromolecules* **2001**, *34*, 7042–7048.
- (47) Abrunhosa, F.; Faria, S.; Gomes, P.; Tomaz, I.; Pessoa, J. C.; Andreu, D.; Bastos, M. *J. Phys. Chem. B* **2005**, *109*, 17311–17319.
- (48) Taira, J.; Jelokhani-Niaraki, M.; Osada, S.; Kato, F.; Kodama, H. *Biochemistry* **2008**, *47*, 3705–3714.

JP804641E